Fracture of random fibre networks with noncentral forces



1990 J. Phys.: Condens. Matter 2 6093

(http://iopscience.iop.org/0953-8984/2/28/001)

J. Phys.: Condens. Matter **2** (1990) 6093–6107. Printed in the UK

# Fracture of random fibre networks with non-central forces

M J Alava† and R K Ritala‡

† Helsinki University of Technology, Department of Technical Physics, SF-02150 Espoo, Finland

‡ Finnish Pulp and Paper Research Institute, PO Box 70, SF-02150 Espoo, Finland

Received 4 August 1989, in final form 28 December 1989

**Abstract.** The breakdown of random networks on triangular lattices is studied numerically. For the interactions the Born Hamiltonian is used, which gives the problem a tensorial character in contrast with the scalar-type random resistor and central force networks. Also, networks built out of fibres of constant length are studied. This gives rise to short-range oriented correlations and a wider binomial distribution for the local elastic moduli. The results show novel effects between the competition of the weakening caused by increased fluctuations in bond strengths and the reinforcement by fibres. These phenomena are studied by averaged breakdown forces, averages over broken bonds during the fracture processes and stress–strain curves. A generic stress–strain curve is presented, which also shows how the tensorial nature of the local interactions reduces the gap between the fracture of random networks and real materials.

## 1. Introduction

Random networks have recently attracted enormous interest as model systems for studying the transport and mechanical properties of disordered solids. The elastic behaviour of random networks consisting of springs is at present well understood in terms of scaling behaviour, even though there exists several universality classes of the elasticity properties.

The breakdown mechanisms of random networks are known only in some simplified cases as fracture, being a dynamical process, is inherently more difficult to study and simulate than elasticity. The breakdown of nearly-complete fuse networks is brittle [1]. Beale and Srolowitz [2] have shown that this brittle breakdown at a low concentration of non-interacting defects carries over to the central force (CF) model. The fracture of very diluted networks near the percolation point is also brittle [3, 4].

There still remains several variables that affect the fracture mechanisms and which have not been studied systematically. Firstly, the fluctuations in the individual bond strength or in the microscopic breakdown threshold affect breakdown [5]. Secondly, the way that the breakdown criterion is imposed can change the fracture behaviour (cf [6]). Thirdly, the microscopic physical model and its symmetry have strong effects on fracture mechanisms.

The few simulation studies of the breakdown mechanics have been as follows: the scalar case either on the fuse networks [7–9] or on the dielectric breakdown of composite

0953-8984/90/286093 + 15 $03.50  

materials [10], the CF model [2, 5, 11], and only very recently the Born model on a square lattice [12] and the beam model [13]. The results together indicate that an appropriate Hamiltonian with bond-bending terms is called for in order to understand the stress–strain curves of real disordered structures.

The complicated processes arising in the fracture of a network in the intermediate-density region between the percolation threshold and the limit of weak disorder are poorly known. In this case the defects interact during the breakdown process, which complicates the relative importance of the mechanisms involved, such as shielding and non-local breakdown [7]. However, for many practical purposes this is the region of major importance.

The simulations and theories worked out so far have assumed that the properties of the bonds in the network are not correlated. However, in composites or in the fibrous network constituting paper, the short-range correlations are very strong. As these correlations are also highly oriented, they are expected to have a major influence on the fracture mechanisms and on the stress–strain curves. One should also note that these materials are true networks and therefore offer an experimental system for verifying the results from the simulations.

In this paper, we report on a first simulation of fracture in random triangular networks with non-central forces. Different densities, ones that are neither close to the percolation threshold nor ordered, are used. We study the effects of short-range correlations which change the local defect geometry. The short-range correlations used here are those that simulate the structure of fibrous materials.

The outline is as follows. In section 2 we introduce the models used, both the ordinary Born model, and our version with short-range correlations. We also describe briefly how the correlations affect the elastic properties. In section 3 we first introduce the simulation methods of fracture. We then study the elastic and plastic behaviour of the networks simulated as a function of damage, the force and the amount of damage needed to fracture and represent averaged stress–strain curves for the simulated cases. In section 4 we conclude with a generic stress–strain curve and summarise the main results.

## 2. The models

### *2.1. Model*

We simulate the fracture of a triangular network, which is the simplest able to carry forces of a tensorial character. For the microscopic description of the medium we use the Born Hamiltonian [14]:

$$H = \tfrac{1}{2}\sum_{i,j} \alpha_{i,j}[(\boldsymbol{u}_i - \boldsymbol{u}_j)\cdot \boldsymbol{k}_\parallel]^2 + \tfrac{1}{2}\sum_{i,j} \beta_{i,j}[(\boldsymbol{u}_i - \boldsymbol{u}_j)\times \boldsymbol{k}_\parallel]^2 \qquad (1)$$

where $\boldsymbol{u}_i$ is the displacement of a lattice node, $\boldsymbol{k}_\parallel$ is a unit vector parallel to the bond between the adjacent nodes $i$ and $j$, and $\alpha_{i,j}$ and $\beta_{i,j}$ are weight factors or the elastic moduli of the bond and the bending stiffness, respectively.

The Born model lacks the rotational invariance [15]. This leads, as the behaviour of the elasticity exponent shows when compared with the rotationally invariant bond-bending model (see, e.g., [16, 17]) ($t_{\mathrm{Born}} \simeq \frac{4}{3}$ and $t_{\mathrm{bb}} \simeq 3.7$), to a stiffer response of the network in the vicinity of the percolation threshold. However, the lack of rotational invariance has less dramatic consequences outside the critical region.

The scalar-type random resistor network (RRN) and the CF model may be recovered from the Hamiltonian by setting $\alpha = \beta$, and $\beta = 0$, respectively. Feng and Sen [18] were

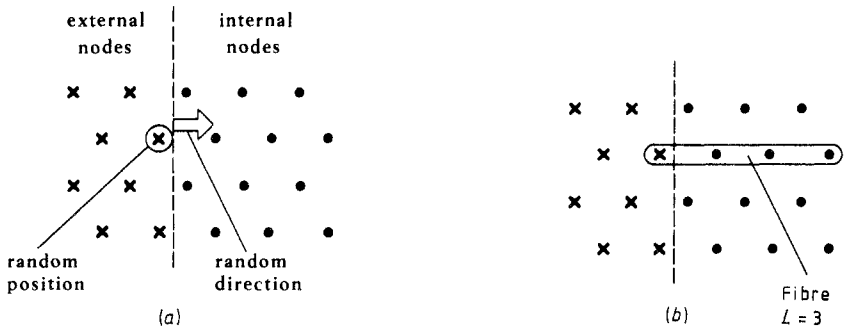


**Figure 1.** The construction of the network out of fibrous elements. (*a*) The end point and the direction are chosen randomly. In addition to the node in the network under consideration we must include external nodes as possible starting points of the fibre to ensure homogeneous density throughout the region of internal nodes. (*b*) A fibre of length 3 placed on the network.

the first to study the elastic crossover as a function of $\beta$; if one increases $\beta$ from zero, the elastic modulus of the network becomes non-zero throughout the region between the rigidity [19] and geometrical thresholds, and satisfies a RRN-type scaling of elasticity near the latter.

To study the effect of interacting defects, i.e. the density region between the critical region and the almost complete network, we construct the network by setting fibrous elements of a given length on the lattice so that both the initial point and the direction are uniformly random (figure 1). When more than one of the objects occupy the same bond of the triangular lattice, the elastic constants associated with that bond are multiplied by the number of the elements. This amounts to considering the elements carrying the load in parallel. In contrast with our procedure, we call the case where the network consists of only singly occupied and unoccupied bonds the ordinary Born model.

We naturally take care of the statistical uniformity of the network by using free boundary conditions in the build-up. Thus, close to the edges, the points outside the final network have to be considered as possible starting points of the fibrous objects. The resulting distribution of the local elastic properties is binomial. The bond-to-bond correlation function of the elastic properties is non-vanishing over distances of the length of the fibrous elements, but only if both the end points of both the bonds lie on the same line.

There are two natural ways of study networks consisting of fibres of different lengths. In particular, when comparing the results with the ordinary Born model, one should study networks with the same amount $p$ of missing bonds:

$$p = 1 - (1 - p_{\text{cover}})^{n_{\text{fibres}}} \tag{2}$$

where $p_{\text{cover}}$ is the probability that a randomly placed fibre covers a bond in the network, and $n_{\text{fibres}}$ is the number of fibres. The method that we have used defines $p_{\text{cover}}$ as

$$p_{\text{cover}} = L/3[N + 2(L - 1)]^2. \tag{3}$$

$N$ is the linear size of the network and $L$ the length of a single fibre. Using the formula for $p_{\text{cover}}$ gives for $n_{\text{fibres}}$:

$$n_{\text{fibres}} = \ln(1 - p)/\ln(1 - p_{\text{cover}}). \tag{4}$$

Another possibility is to consider the average modulus:

$$K_{\text{ave}} = \alpha n_{\text{fibres}} p_{\text{cover}}. \tag{5}$$

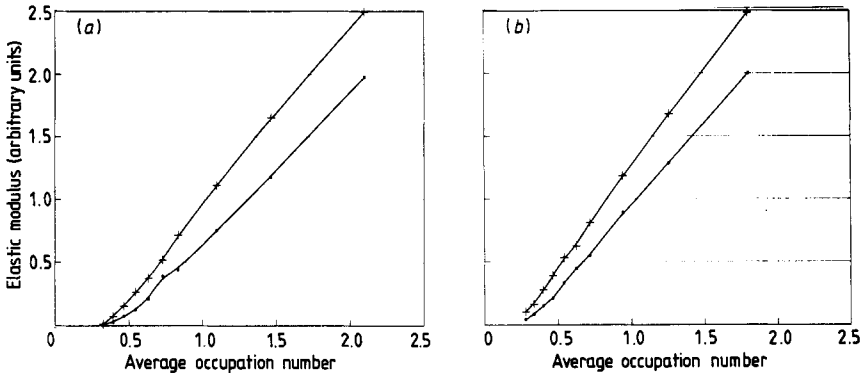


**Figure 2.** The elastic modulus of a 20 × 20 fibrous network as a function of the average occupation number of a bond in the lattice for (*a*) a fibre length $L$ of 2 and (*b*) a fibre length $L$ of 4: ●, $\beta/\alpha = 0.1$; ×, $\beta/\alpha = 0.4$.

In the limit of large networks, $K_{ave}$ and $p$ are monotonically related to each other:

$$\lim_{N\to\infty} p \to 1 - \exp(-K_{ave}/\alpha). \tag{6}$$

Owing to finite size effects the actual effective length of a fibrous element is smaller than its nominal value and can be given as a function of network size and nominal length. Starting from the effective length of a fibre of length $L$ on a strip of bonds of length $N$, one arrives at the formula

$$L_{eff} = ((N - L)L + \sum_{i=1}^{L-1} 2i)/N + L - 2. \tag{7}$$

If geometrical factors are taken into account (i.e. the shape of the network) together with equation (7), a rather complicated expression results The effective lengths used in this study are 1.00, 1.87 and 3.30 for $L = 1$, $L = 2$ and $L = 4$, respectively, which shows that for practical purposes $L \ll N$.

### *2.2. Elasticity*

Although the addition of longitudinal short-range correlations changes the percolation threshold, one can by simple scaling arguments show that in the critical region the scaling of the elastic modulus is the same as that of the ordinary Born model. This can also be seen from our numerical simulations. Figure 2 shows that outside the critical region the elastic modulus is a rather linear function of the average elastic modulus. The critical region judged by this parameter gets smaller as the length of the fibrous elements increases. However, figure 3 shows that, when we study the elastic modulus as a function of the probability that a given bond is missing instead of the average elastic modulus, we find a behaviour similar to the ordinary Born model. As the two quantities are linearly related close to the percolation threshold, we conclude that critical exponents in terms of these two quantities are the same.

We do not try to give a complete account of the effects that the correlations have on the backbone. However, these can be discussed to some extent with the help of arguments

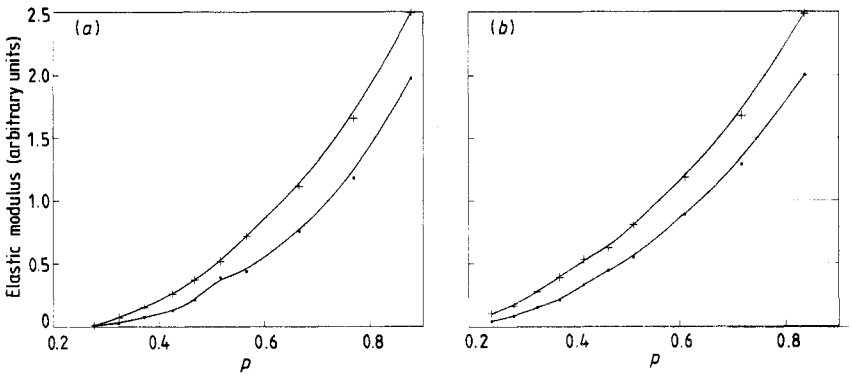


**Figure 3.** The (*a*) $L = 2$ data and (*b*) $L = 4$ data of figure 2 as a function of the probability $p$ that a bond is occupied by at least one fibre.

concerning the coordination number of a node in the network and the geometry of longitudinal holes, i.e. the cluster statistics of missing bonds. With a constant bond elastic modulus, i.e. the ordinary Born model, the coordination number is binomially distributed with a mean of $6p$. In the case of a network of fibrous elements we construct the probabilities of different coordination numbers from the probabilities describing the contributions from each of the axes.

Denoting the probability that the coordination number $c_{\text{axis}}$ along an axis is zero by $P_0$ one by $P_1$ and two by $P_2$, we have for the $P_i$-values

$$P_0 = P(n = 0)^2 \tag{8}$$

$$P_1 = 2P(n = 0)P(n > 0) \tag{9}$$

$$P_2 = 1 - P_0 - P_1 \tag{10}$$

where $P(n = m)$ is the conditional probability for the elastic modulus $n$ of a bond to be $m$ if the neighbouring two bonds are not covered simultaneously by one or more fibres. Expressing this probability by $1 - p_{\text{cond}}$, $P(n = 0)$ is

$$\{1 - p_{\text{cover}}/[L - (L - 1)p_{\text{cover}}]\}^{n_{\text{fibres}}} \tag{11}$$

and

$$\{1 - [(L - 1)/L]p_{\text{cover}}\}^{n_{\text{fibres}}} \tag{12}$$

denotes $1 - p_{\text{cond}}$; $p_{\text{cover}}$ has been introduced in equation (3). $P(n > 0)$ can be, of course, expressed as $1 - P(n = 0)$.

By using the $P_i$-values, we arrive at figure 4, where the probabilities for different coordination numbers $c$ are given as functions of $p$ and $L$. Comparing the different distributions, the effects of fibrousness can be seen most clearly in the diluted cases (i.e. $p = 0.7$ and $p = 0.5$). When $p$ is close to unity, increasing the fibre length gradually reduces the proportion of nodes with $c = 5$ and increases that with $c = 4$. When $p = 0.7$ the trend continues, with longer fibres favouring even coordination numbers. Finally, when $p = 0.5$, a comparison between, for example, the $L = 4$ and $L = 1$ distributions shows how the value of $P_3$ becomes smaller as the length increases which causes a larger amount of lattice nodes to have either $c = 6$ or $c = 0$ while the probabilities $P_1$, $P_2$, $P_4$ and $P_5$ do not change very much.

The effects of fibrousness on the backbone are thus due to a strengthening effect caused by a reduction in 'dangling ends', i.e. there are fewer bonds that do not contribute

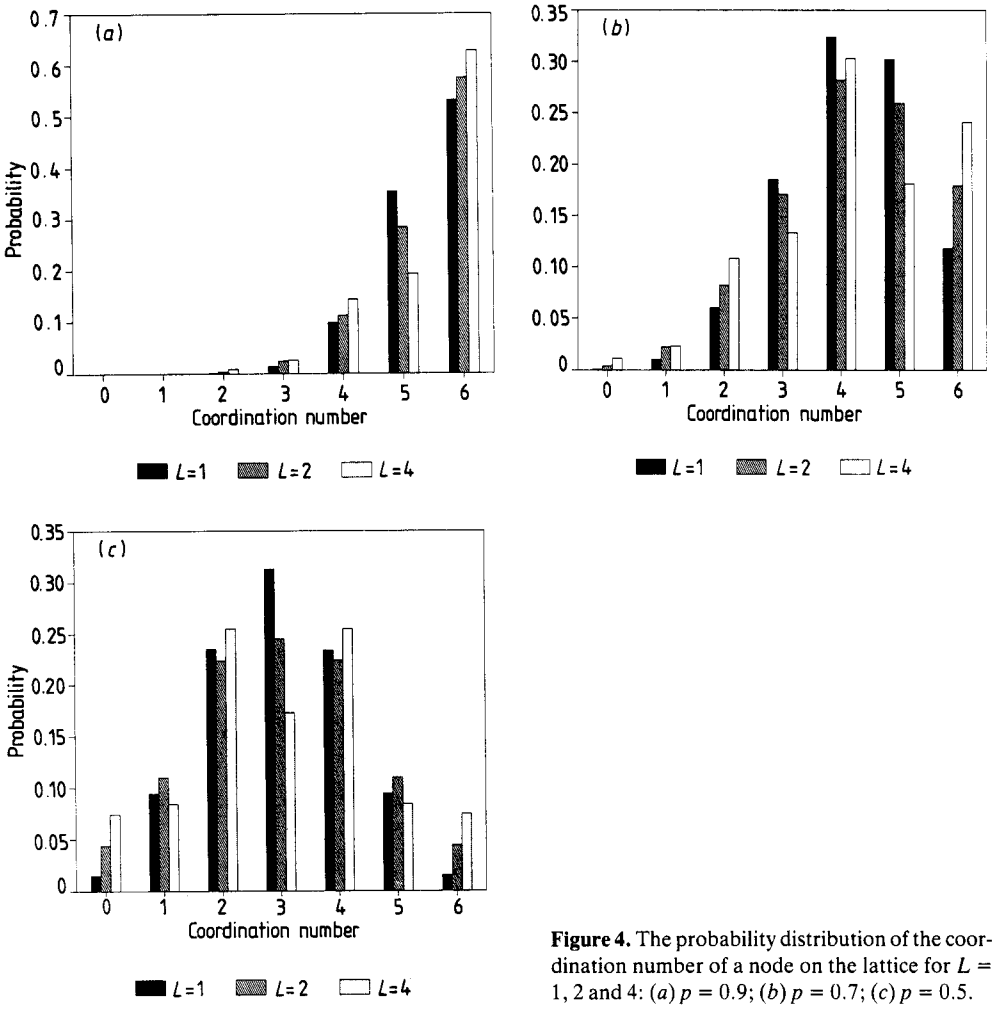


**Figure 4.** The probability distribution of the coordination number of a node on the lattice for $L$ = 1, 2 and 4: (*a*) $p = 0.9$; (*b*) $p = 0.7$; (*c*) $p = 0.5$.

to the elastic modulus and so do not belong to the backbone of the network. Bonds adjacent to a node with an odd coordination number have also on average a smaller elastic modulus. This will lead to enhanced interaction between fibres parallel to the external strain and also larger parallel defects.

Fibrousness also affects the distribution of the bond forces when the network is elongated. The critical types of defect in the high-density regime have been studied in the context of fuse networks [20–24] and the CF model [2], and their differences imply new effects in this case, too. Additional effects arise from the combination of longitudinal correlations and the tensorial character of mechanical forces, which emphasises the non-local fracture behaviour compared with other scalar or tensorial models.

## 3. Numerical results

### *3.1. Simulation method*

To simulate fracture, we use the semi-dynamical method (see, e.g., [8]). First, a random network with the chosen fibre length and probability $1 - p$ for a bond to be missing from

the network is generated. Then the network is strained by a constant amount and the corresponding force is calculated. All the individual bonds in the lattice are considered for breakdown by the selected criterion, and the most affected is broken. To generate the stress–strain curve of the network, the stress and strain are rescaled so that the broken bond is, in our case, strained to the critical length. This process is repeated until the network breaks down and becomes disconnected.

We studied three probabilities: $p = 0.9$, $p = 0.7$ and $p = 0.5$. The fibre lengths considered were $L = 1$, $L = 2$ and $L = 4$, and the results were compared also with the ordinary Born model. The calculations were performed on a VAX 11/750 with a floating point accelerator. Typical CPU time needed to complete a run of ten samples of each of the probabilities, two $\beta$-values and one fibre length was of the order of 15 h for $20 \times 20$ networks. The connectivity matrix in the force equation of the network was inverted by a standard library subroutine for sparse band matrix inversion.

The dynamics of the fraction depend on the fracture criterion. One might consider the energy stored in the bond, the force acting upon it, the strain or the corresponding moment, or a combination of these. The selection is by nature somewhat arbitrary, and that used here was the computationally simplest although somewhat unphysical. We use the criterion for the strain of an individual bond. When the $\beta$-to-$\alpha$ ratio is close to unity, this should lead to similar results as with a force or energy criterion. To study the effect of this choice combined with the rotationally non-invariant Hamiltonian, we use two values for the $\beta$-to-$\alpha$ ratio: 0.1 and 0.4.

We average the network responses in a way which is mathematically equivalent to considering the responses of the individual networks by straining them in parallel. Given for a network $i$ the corresponding bond-breaking strengths $F(i, j)$ and elongations $E(i, j)$, the combined effect of $n$ parallel networks results in a stress–strain curve defined by the elastic modulus $Y$ as

$$Y(\delta) = \langle F(k, l)/E(k, l) \rangle \tag{13}$$

where the average is performed over all the networks, $\delta$ is an 'averaged elongation' and the $F(k, l)$ and $E(k, l)$ are taken such that $l$ corresponds to the smallest $E$ larger than $\delta$. This idea is clearly consistent with the idea of stretching a sample continuously and monitoring the force needed. In the literature there exists already another averaging method [11]; however, that presented here seems to us to be more physical.

### *3.2. Breakdown statistics*

To illustrate how the breakdown process depends on the parameters $p$, $L$ and $\beta/\alpha$, we first discuss the effect of partial fracture on the static, or elastic, response of a network. Then we compare the following properties of the fracture processes:

(i) the maximum force that the lattice can support;

(ii) the number of bonds broken in the fracture;

(iii) 'clustering' of bonds in fracture (that is, as the elongation of the network is increased monotonically, bonds may break at the same value);

(iv) the average modulus of broken bonds during the fracture.

*3.2.1. Static behaviour.* In figure 5 we show some typical examples of the elastic moduli as functions of the number of broken bonds. These curves appear rather similar in contrast with the great differences in stress–strain curves in section 3.3. The only trend seems to be the slower reduction in network modulus at the beginning of the fracture in

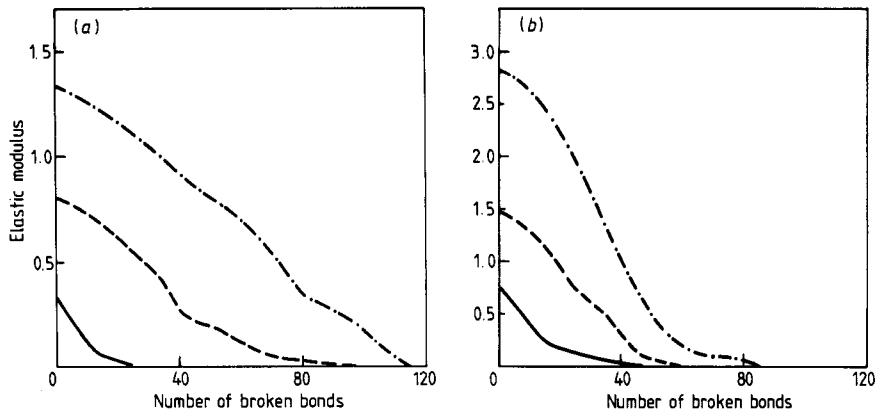


**Figure 5.** The average elastic modulus of a network as a function of bond broken during the fracture for $p = 0.9$ (– · –), $p = 0.7$ (– – –) and $p = 0.5$ (——): (*a*) ordinary Born model; (*b*) $L = 4$.

the case of fibrous networks. One should remember that in many cases the maximum force is reached rather early in terms of bonds broken during the fracture.

An approximate explanation for the behaviour of the elastic modulus can be given by different phases in the elastic response of a network. At the beginning of the fracture, bonds with a small individual elastic modulus are most susceptible to breakdown. However, their contribution to the elastic modulus of the network is not so large owing to their small modulus. As the fracture continues, bonds with a larger elastic modulus start to break. This also influences the modulus of the whole network indirectly because clumps of bonds may be disconnected from carrying the load and thus do not contribute to the elastic modulus. In some cases the behaviour of the average modulus is almost linear down to the final fracture. This results from the network's becoming essentially a system of non-interacting strings connected in parallel. When one of these strings breaks, the elastic modulus of the remaining network is decreased in a linear fashion.

*3.2.2. The breakdown forces.* There are two basic approaches to the process of fracture. One can control the process either by force or by elongation. We have chosen the latter, because it includes also information on force-controlled breakdown. In addition, we gain insight about the final phase of the fracture. We have calculated the maximum forces during the breakdown processes together with the forces needed to break the first bond and the last bond (see table 1). As the average modulus of a bond changes as a function of $p$, we have presented these data also normalised by the expectation value of the modulus at a bond (equation (5)) (table 2).

Increasing the $\beta$-to-$\alpha$ ratio has a strong influence on the magnitude of the forces. With a small ratio, local movements perpendicular to the original direction of the bond are favoured energetically. This kind of shear leads to the breakdown of such bonds, as they are readily stretched beyond the criterion used. A partial reason is also the extra energy needed to deform the network when $\beta$ is larger, proportional to the change $\delta\beta$ in $\beta$.

The difference between fibrous and non-fibrous networks is most pronounced when $p$ is small. At $p = 0.5$ the average forces needed for fracture differ from each other considerably, if the fibre length is increased from $L = 1$ to $L = 2$. These cases differ also considerably from the ordinary Born model (note, however, that $K_{ave}$ for the ordinary

**Table 1.** Unnormalised breakdown forces for the ordinary Born model and different fibre lengths. In the second column are the forces needed to break the first bond, in the third the forces to break the last bond to disconnect the network and in the fourth the maximum force.

| $p$ | $F_i$ | $F_l$ | $F_m$ |
|---|---|---|---|
| | $K = 1, \beta = 0.1$ | | |
| 0.9 | 0.733 | 0.061 | 0.959 |
| 0.7 | 0.292 | 0.016 | 0.403 |
| 0.5 | 0.067 | 0.016 | 0.084 |
| | $K = 1, \beta = 0.4$ | | |
| 0.9 | 1.436 | 0.108 | 1.628 |
| 0.7 | 0.692 | 0.069 | 0.834 |
| 0.5 | 0.227 | 0.053 | 0.251 |
| | $L = 1, \beta = 0.1$ | | |
| 0.9 | 1.006 | 0.063 | 1.210 |
| 0.7 | 0.299 | 0.041 | 0.368 |
| 0.5 | 0.052 | 0.016 | 0.057 |
| | $L = 1, \beta = 0.4$ | | |
| 0.9 | 1.854 | 0.207 | 1.928 |
| 0.7 | 0.623 | 0.089 | 0.707 |
| 0.5 | 0.196 | 0.055 | 0.196 |
| | $L = 2, \beta = 0.1$ | | |
| 0.9 | 1.121 | 0.136 | 1.427 |
| 0.7 | 0.379 | 0.025 | 0.483 |
| 0.5 | 0.122 | 0.028 | 0.128 |
| | $L = 2, \beta = 0.4$ | | |
| 0.9 | 2.086 | 0.350 | 2.269 |
| 0.7 | 0.977 | 0.092 | 1.024 |
| 0.5 | 0.307 | 0.065 | 0.315 |
| | $L = 4, \beta = 0.1$ | | |
| 0.9 | 1.492 | 0.132 | 1.937 |
| 0.7 | 0.679 | 0.062 | 0.796 |
| 0.5 | 0.268 | 0.034 | 0.294 |
| | $L = 4, \beta = 0.4$ | | |
| 0.9 | 2.253 | 0.190 | 2.697 |
| 0.7 | 1.284 | 0.167 | 1.388 |
| 0.5 | 0.480 | 0.088 | 0.543 |

Born model is different from that of fibrous networks at given $p$). The strength decreases considerably when a wider binomial distribution is introduced. The difference between the force to break the first bond, and the breakdown force, gets smaller, too. This can be attributed to the so-called 'path formation' [5], in which the breakdown process proceeds locally by seeking the weakest bonds and thus tries to avoid the stronger backbone of a network.

Normalisation of the results reveals the tendencies discussed above even more strikingly. A wider bond moduli distribution ($L = 1$) results in an increasing weakness with lower values of $p$.

Fibres of length larger than unity have two effects. At high densities, the binomial distribution dominates, and the normalised maximum forces are smaller than in the ordinary Born model. At lower densities, a strengthening effect appears. This is because

**Table 2.** Forces in table 1 normalised by the expectation value of the bond elastic modulus.

| $p$ | $F_i$ | $F_l$ | $F_m$ |
|---|---|---|---|
| | $K = 1, \beta = 0.1$ | | |
| 0.9 | 0.733 | 0.061 | 0.959 |
| 0.7 | 0.292 | 0.016 | 0.403 |
| 0.5 | 0.067 | 0.016 | 0.084 |
| | $K = 1, \beta = 0.4$ | | |
| 0.9 | 1.436 | 0.108 | 1.628 |
| 0.7 | 0.692 | 0.069 | 0.834 |
| 0.5 | 0.227 | 0.053 | 0.251 |
| | $L = 1, \beta = 0.1$ | | |
| 0.9 | 0.393 | 0.024 | 0.473 |
| 0.7 | 0.174 | 0.023 | 0.214 |
| 0.5 | 0.024 | 0.011 | 0.041 |
| | $L = 1, \beta = 0.4$ | | |
| 0.9 | 0.725 | 0.081 | 0.754 |
| 0.7 | 0.362 | 0.052 | 0.411 |
| 0.5 | 0.141 | 0.040 | 0.141 |
| | $L = 2, \beta = 0.1$ | | |
| 0.9 | 0.438 | 0.053 | 0.558 |
| 0.7 | 0.220 | 0.014 | 0.281 |
| 0.5 | 0.088 | 0.020 65 | 0.092 |
| | $L = 2, \beta = 0.4$ | | |
| 0.9 | 0.816 | 0.137 | 0.888 |
| 0.7 | 0.568 | 0.054 | 0.596 |
| 0.5 | 0.221 | 0.047 | 0.227 |
| | $L = 4, \beta = 0.1$ | | |
| 0.9 | 0.584 | 0.051 | 0.758 |
| 0.7 | 0.395 | 0.036 | 0.463 |
| 0.5 | 0.194 | 0.025 | 0.212 |
| | $L = 4, \beta = 0.4$ | | |
| 0.9 | 0.882 | 0.074 | 1.055 |
| 0.7 | 0.747 | 0.097 | 0.807 |
| 0.5 | 0.347 | 0.063 | 0.392 |

in very dilute networks the effect of local correlations on the structure of the backbone overcomes weaknesses induced by fluctuations in bond elastic moduli.

Earlier results in fracture are in some contrast with those presented above. In the CF model it has been concluded by Sahimi and Goddard [5] that, when the disorder is introduced in the mechanical properties of the bonds, the fracture is brittle ($f_i \simeq f_m$), which seems to hold in our case at $L = 1$. Also, Hassold and Srolovitz [12] have proposed on the basis of simulations with the ordinary Born model on a square lattice that in practice this relation is at least an excellent approximation. The applicability of the former idea in our case is dubious, as the addition of a bond-bending part to the Hamiltonian network most probably affects the fracture mechanism. The latter idea invokes doubts about the right underlying geometry of the network for study of fracture. It is well known that the elastic threshold of a square lattice, with CF springs, in terms of $p$ is unity and the crossover is dominant in a large region of $\beta$ [18].

*3.2.3. Damage needed to fracture.* A wide distribution of the bond elastic moduli leads to easy path formation and thus reduces the number of broken bonds needed to disconnect a

**Table 3.** Numbers of bonds broken on average during the fracture and the 'cluster sizes', i.e. numbers of bonds broken for each increase in strain.

| $p$ | Average amount | Cluster size |
|---|---|---|
| | $K = 1, \beta = 0.1$ | |
| 0.9 | 99.4 | 6.58 |
| 0.7 | 77.6 | 3.59 |
| 0.5 | 19.0 | 2.53 |
| | $K = 1, \beta = 0.4$ | |
| 0.9 | 96.8 | 11.66 |
| 0.7 | 63.5 | 4.54 |
| 0.5 | 14.0 | 2.55 |
| | $L = 1, \beta = 0.1$ | |
| 0.9 | 42.4 | 6.00 |
| 0.7 | 21.5 | 6.10 |
| 0.5 | 7.8 | 3.40 |
| | $L = 1, \beta = 0.4$ | |
| 0.9 | 37.6 | 3.50 |
| 0.7 | 19.9 | 3.90 |
| 0.5 | 7.3 | 2.90 |
| | $L = 2, \beta = 0.1$ | |
| 0.9 | 47.5 | 7.54 |
| 0.7 | 40.3 | 3.30 |
| 0.5 | 14.6 | 2.60 |
| | $L = 2, \beta = 0.4$ | |
| 0.9 | 50.1 | 7.05 |
| 0.7 | 26.5 | 6.02 |
| 0.5 | 12.3 | 3.42 |
| | $L = 4, \beta = 0.1$ | |
| 0.9 | 54.2 | 5.89 |
| 0.7 | 40.8 | 4.98 |
| 0.5 | 22.5 | 2.92 |
| | $L = 4, \beta = 0.4$ | |
| 0.9 | 69.7 | 5.49 |
| 0.7 | 46.1 | 5.42 |
| 0.5 | 23.1 | 3.30 |

network. The fibrous structure on the other hand reinforces the network locally because the curve of rupture has to be longer to find a weak path. This is more pronounced at low densities. Then in the network with $L = 4$ the number of bonds broken exceeds that of the ordinary Born model (table 3).

The degree of brittleness, i.e. whether the fracture occurs in few sequences or more continuously, is another classifying property of the breakdown processes. We find that in the breakdown of networks of fibrous structure the process happens in smaller steps close to $p = 1.0$. The average number of steps in fracture indicates that the non-fibrous network fractures in a less brittle fashion. As the local network geometry becomes more random, the differences get smaller in terms of the size of clusters in the process. There seems to be a qualitative deviation in the fracture mechanisms between the cases $L = 2$ and $L = 4$ at low densities. This shows how the degree of reinforcement affects the

**Table 4.** Average occupation numbers of bonds broken during the fracture.

| $p$ | Occupation number |
|---|---|
| | $L = 1, \beta = 0.1$ |
| 0.9 | 2.03 |
| 0.7 | 1.41 |
| 0.5 | 1.14 |
| | $L = 1, \beta = 0.4$ |
| 0.9 | 1.70 |
| 0.7 | 1.18 |
| 0.5 | 1.04 |
| | $L = 2, \beta = 0.1$ |
| 0.9 | 2.03 |
| 0.7 | 1.46 |
| 0.5 | 1.27 |
| | $L = 2, \beta = 0.4$ |
| 0.9 | 1.84 |
| 0.7 | 1.30 |
| 0.5 | 1.10 |
| | $L = 4, \beta = 0.1$ |
| 0.9 | 2.19 |
| 0.7 | 1.53 |
| 0.5 | 1.24 |
| | $L = 4, \beta = 0.4$ |
| 0.9 | 2.09 |
| 0.7 | 1.49 |
| 0.5 | 1.19 |

brittleness, as the former fracture in a brittle fashion in contrast with the latter. These results are based on rather restricted information and are therefore tentative. Qualitatively similar results in terms of $\beta$-to-$\alpha$ ratio dependence have been achieved by Hassold and Srolovitz [12], except in the $L = 4$ case, where taking the limit $\beta \rightarrow \alpha$ does not seem to lead to a reduction in the number of bonds broken.

From the statistics of the occupation numbers of broken bonds we find the following features (table 4). Firstly, the $\beta$-to-$\alpha$ ratio clearly affects the average modulus. This is because, when a bond is stretched in a direction perpendicular to its original, the bond's modulus matters less. Comparing the results with the average elastic moduli corresponding to the densities (2.56, 1.72 and 1.38 for $p = 0.9, 0.7$ and 0.5), we see that the average number of the broken bonds increases as a function of fibre length and becomes finally close to the value of the ordinary Born model (i.e. unity). Also, the difference between the two $\beta$-cases diminishes. Therefore, we conclude that at lower densities the bond strength fluctations are of less importance than the intrinsic reinforcing due to fibres.

### *3.3. Stress–strain curves*

From the experimental point of view the most interesting aspect in our numerical calculations are the stress–strain curves, which are the only kind of simulation data that can be readily compared with the behaviour of real materials. In figures 6–11 we display the calculated stress–strain curves averaged as explained in section 3.1.

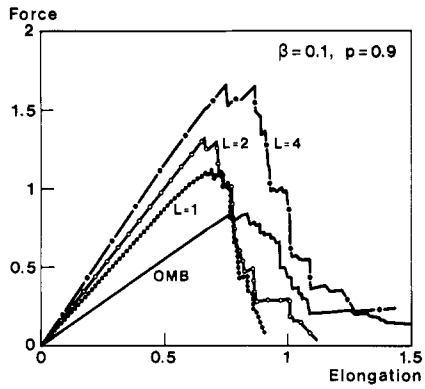


**Figure 6.** Averaged stress–strain curves (for the averaging method see text) at $\beta/\alpha = 0.1$ and $p = 0.9$. The curves show the behaviour for the ordinary Born model (——) and $L = 1$. (●●●), $L = 2$ (—○—) and $L = 4$ (—●—).

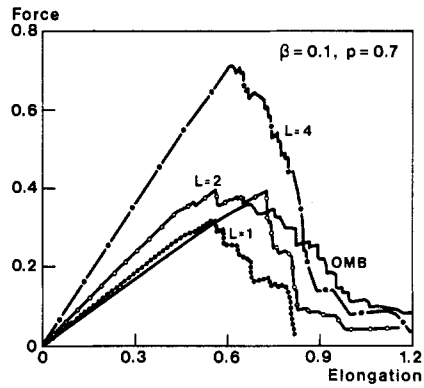


**Figure 7.** Averaged stress–strain curves at $\beta/\alpha = 0.1$ and $p = 0.7$. The symbols are as in figure 6.

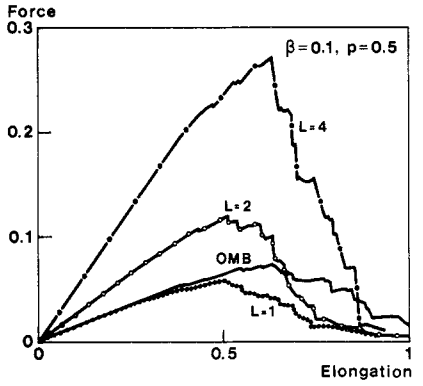


**Figure 8.** Averaged stress–strain curves at $\beta/\alpha = 0.1$ and $p = 0.5$. The symbols are as in figure 6.

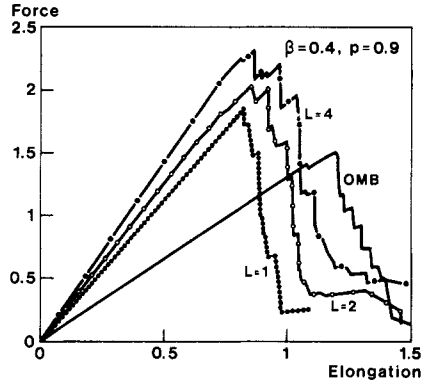


**Figure 9.** Averaged stress–strain curves at $\beta/\alpha = 0.4$ and $p = 0.9$. The symbols are as in figure 6.

The fibrous networks ($L = 2, 4$) fracture qualitatively in the same fashion at all values of $p$ even though the force scales differ from each other. A few weak bonds break well before the maximum force and corresponding elongation. Later during the fracture the response remains very similar to an undamaged network in a quite large region; the length of this plastic region increases with decreasing $p$. The major fracture occurs rather rapidly compared with the ordinary Born model, but even after that the value of the elastic modulus does not become zero and the elongation can be increased further.

With fibre length $L = 1$ the fracture is rather different. The degree of dilution has a strong effect. When $p$ is close to unity, the breakdown behaviour is brittle, as is to be expected from earlier results [2, 12]. There is, however, a clear difference between the ordinary Born model and the $L = 1$ case in the remaining strength as the elongation is increased after the maximum stress has been reached. This again indicates the formation of a short path of fracture when weaker bonds exist.

At lower densities a plastic region appears close to the breakdown force and corresponding elongation. In this region the elastic modulus decreases from its original

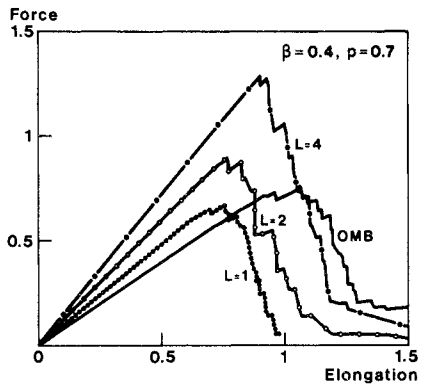


**Figure 10.** Averaged stress–strain curves at $\beta/\alpha = 0.4$ and $p = 0.7$. The symbols are as in figure 6.

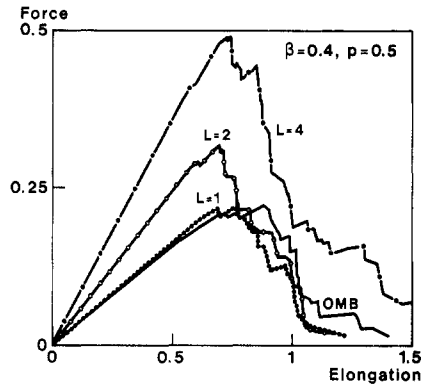


**Figure 11.** Averaged stress–strain curves at $\beta/\alpha = 0.4$ and $p = 0.5$. The symbols are as in figure 6.

value before the onset of fracture. The importance of this region grows as $p$ gets smaller and consequently the features of brittleness vanish. The difference between the ordinary Born model and the $L = 1$ case is still present when $p = 0.7$, as the very different behaviour shows. The stress of the more heterogeneous network increases more rapidly at the beginning as its average elastic modulus is larger, but the final fracture occurs well before that of the ordinary Born model. Finally, when $p = 0.5$ the curves almost coincide in shape, which is to be expected as the bond elastic modulus distribution of the $L = 1$ case becomes narrower.

The effect of fibre length is clearly distinguishable in all of the examples presented. At $p = 0.9$, increasing the length does not have very large quantitative consequences; only the stress to strain a network for a given amount gets larger. As indicated earlier, the qualitative difference between the $L = 2$ and $L = 4$ cases is small at all values of $p$. Only the force scales start to differ from each other. This effect grows with smaller $p$ and seems to depend on the $\beta$-to-$\alpha$ ratio, too. In conclusion, the fibre length does not increase the maximum strain that the network can bear, but the stress. This is due to the strengthening effect of the fibres on the backbone, which keeps the network more intact for a given elongation. The elongation corresponding to the maximum force in the cases of the ordinary Born model is usually larger than that of fibrous models. This results from the lack of local fluctuations.

## 4. Summary and discussion

We present here a phenomenological model for the stress–strain curves of the types of network discussed in this paper. In the first phase, with modest elongation, no damage occurs and the network can be strained reversibly. In the second phase, when the network is strained above a threshold value, the weakest bonds in the lattice start to break. However, the effect due to this on the ability of the network to carry load is negligible. In the third phase, even stronger bonds start to break. Consequently, the stress saturates which results from a gradual geometrical reorganisation of the network.

The length of the saturation phase in terms of strain depends on the microscopic properties of the network. Increasing disorder, i.e. lower $p$, makes the saturation phase longer. The length of the regime depends also inversely on the fibre length. Brittle

behaviour in stress–strain is to be expected when the backbone of the network is rigid, i.e. in the fracture of uniform nearly complete networks and in that of the diluted fibrous networks.

Finally there follows the phase of major fracture, in which large regions become only singly connected to the backbone of the network and are thus unable to carry load. The stress decreases rapidly which is partially due to the missing rotational invariance of the Born Hamiltonian. Rotating groups of bonds without increasing the energy stored in internal deformation can cause the breakdown of the bonds connecting them to the main body of the backbone, which reduces the elastic modulus of the network greatly. In the final region, the weak links connecting the network are broken.

To conclude, the results indicate competition between path-forming and screening and possibly also non-local breakdown. The first phenomenon is due to fluctuations in individual bond strengths and the latter to microscale correlations from fibres of non-unity length. Even a minor change in the bond length is able to affect the breakdown characteristics of random networks in a profound way. The character of the breakdown problem resulting from the Born Hamiltonian gives a clearly better description of real materials than the usual RRN and CF models do.

## References


[1] Duxbury P M, Beale P L and Leath P D 1986 *Phys. Rev. Lett.* **57** 2052
Duxbury P M, Leath P D and Beale P L 1987 *Phys. Rev.* B **36** 367
[2] Beale P D and Srolovitz D J 1989 *Phys. Rev.* B **37** 5500; 1985 *Phys. Rev.* B **32** 4607
[3] Coniglio A 1981 *Phys. Rev. Lett.* **46** 250
[4] For an application of the nodes–links–blobs picture to fracture, see Sornette D 1987 *Phys. Rev.* B **36** 8847
[5] Sahimi M and Goddard J D 1986 *Phys. Rev.* B **33** 7848
[6] Sornette D 1987 *J. Physique* **48** 1843
[7] Gilabert A, Vanneste C, Sornette D and Guyon E 1987 *J. Physique* **48** 763
[8] de Arcangelis L, Redner S and Herrmann H J 1985 *J. Physique Lett.* **46** L-585
[9] Kahng B, Batrouni G G, Redner S, de Arcangelis L and Herrmann H J 1988 *Phys. Rev.* **37** 7625
[10] Beale P D and Duxbury P M 1988 *Phys. Rev.* B **37** 2785
[11] Hansen A, Roux S and Herrmann H J 1989 *J. Physique* **50** 733
[12] Hassold G N and Srolovitz D J 1989 *Phys. Rev.* B **39** 9273
[13] Herrmann H J, Hansen A and Roux S 1989 *Phys. Rev.* **39** 637
[14] Born M and Huang K 1954 *Dynamical Theory of Crystal Lattices* (Oxford: Oxford University Press)
[15] Keating P N 1966 *Phys. Rev.* **152** 774
[16] Feng S, Sen P N, Halperin B I and Lobb C J 1984 *Phys. Rev.* B **30** 5386
Schwartz L M, Feng S, Thorpe M F and Sen P N 1985 *Phys. Rev.* B **32** 4607
[17] Sahimi M 1986 *J. Phys. C: Solid State Phys.* **19** L79
[18] Feng S and Sen P N 1984 *Phys. Rev. Lett.* **52** 216
[19] Day A R, Tremblay R R and Tremblay A-M S 1986 *Phys. Rev. Lett.* **56** 2501
Feng S, Thorpe M F and Garboczi E J 1985 *Phys. Rev.* B **31** 276
[20] Machta J and Guyer R A 1986 *Phys. Rev.* B **35** 2142
[21] Li Y S and Duxbury P M 1987 *Phys. Rev.* B **36** 5411
[22] Chan S K, Machta J and Guyer R A 1989 *Phys. Rev.* B **39** 9236
[23] Helsing J, Axell J and Grimwall G 1989 *Phys. Rev.* B **39** 9231
[24] Li Y S and Duxbury P M 1988 *Phys. Rev.* B **38** 9257